Contemporary Mathematics

Numerical aspects of sonic-boom minimization

Navid Allahverdi, Alejandro Pozo, and Enrique Zuazua

Abstract. The propagation of the sonic-boom produced by supersonic aircrafts can be modeled by means of a nonlocal version of the viscous Burgers equation. In this paper, motivated by the sonic-boom minimization problem, we analyze the numerical aspects of the optimization process, with a focus on the large-time dynamics of the underlying model. We develop an adjoint methodology at the numerical level allowing to recover accurate approximations of the minimizers. We observe however that some of the minima are hard to achieve due to the intrinsic nonlinear and viscous effects.

1. Motivation

1.1. Sonic-boom minimization. When flying above the speed of sound, supersonic airplanes create pressure disturbances in the atmosphere resulting from air compression due to the moving volume of the plane and the aerodynamic lift, which is required to maintain the flight altitude. Some portion of the pressure disturbances, which imply a significant amount of acoustic energy, propagates in the atmosphere and reaches the ground level, resulting in the so-called sonic-boom [**2**]. Sonic-boom, perceived on the ground as two subsequent loud bangs with a short time lapse in between, is annoying for people living in the sonic-boom carpet under the flight track and may potentially damage building facade and glazing in extreme cases. For all these reasons sonic-boom has been one of the main obstacles when it comes to commercializing supersonic air travels.

Throughout the last decades of the 20th century, it became clear that sonic-boom reduction technologies had to be advanced, in order to make flights of supersonic airplanes a reality. In fact, the DARPA/NASA/Northrop-Grumman Shaped Sonic Boom Demonstrator (SSBD) project [**12**] showed that the sonic-boom could be partially mitigated by tailoring the shape of the aircraft, confirming it experimentally for the first time.

2010 *Mathematics Subject Classification.* 49M25, 35Q35, 35B40.

This research is supported by the Advanced Grant NUMERIWAVES/FP7-246775 of the European Research Council Executive Agency, FA9550-14-1-0214 of the EOARD-AFOSR, FA9550-15-1-0027 of AFOSR, the BERC 2014-2017 program of the Basque Government, the MTM2011-29306 and SEV-2013-0323 Grants of the MINECO and a Humboldt Award at the University of Erlangen-Nürnberg. A. Pozo is also supported by the Basque Government (PREDOC Program 2012, 2013 and 2014).

In this paper, we confine ourselves to the simulation of the propagation of the sonic-boom from the near-field of the plane down to the ground level. We refer the reader to [**2**] for a detailed review on the state of the art regarding the complete sonic-boom minimization problem, including shape optimization of the aircraft as well.

It is well known that the pressure signature evolves into an N-wave (see Figure 1) if the time of propagation is long enough. The N-wave refers to the shape that results from the collapse of the multiple shocks into a leading and a trailing shock separated by a nearly linear pressure expansion, perceived by humans as the aforementioned sonic-boom. At the beginning, it was thought that the N-wave was unavoidable. But McLean proved theoretically that it was possible to tailor the near-field signature of the aircraft so that the N-wave was not developed by the time the signature had reached the ground level [**9**], thus, mitigating the sonic-boom. Nevertheless, as mentioned above, this was not empirically verified until the SSBD tests was done in 2003.

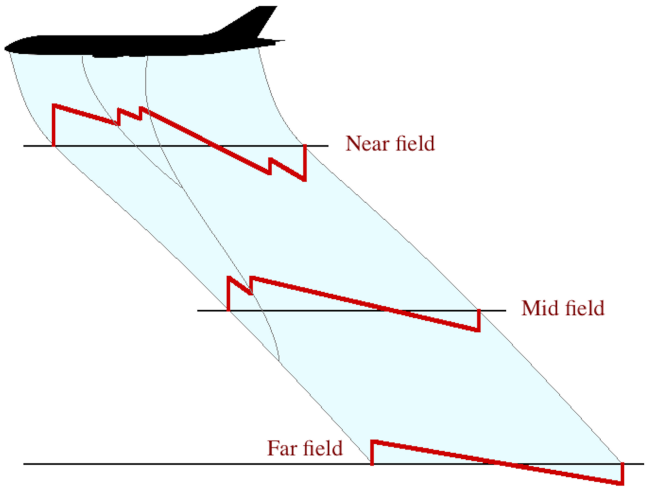

FIGURE 1. Diagram of the propagation of the sonic-boom. Shocks created in the near-field collapse into two single shocks, forming an N-wave in the far-field.

The high cost of realistic experiments like the SSBD project promoted the development of theoretical and computational tools that could handle the simulation of sonic-boom minimization problem more efficiently. Historically, linear theory was used to model the sonic-boom propagation, following the seminal works done by Hayes [**6**] and Whitham [**18**] in the late 1940s and early 1950s and, until recently, most of the analytical and numerical research done followed that path.

More recently, new nonlinear physical models have been utilized to improve the sonic-boom propagation from the near-field to the ground. Two such methods are worth to mention. One approach, proposed by Ozcer [**11**], advocates the use of the full potential equation in the region from the near-field to the ground. The

other approach, adopted initially by Cleveland [**5**] and then by Rallabhandi [**16**], uses an augmented Burgers equation within the context of ray-tracing/geometrical acoustics to propagate the source signatures to the ground, including viscous effects that lead to shock discontinuities with non-zero thickness.

1.2. The augmented Burgers equation (ABE). In this paper we focus on the latter approach. The augmented Burgers equation –or extended Burgers equation [**5**]– takes into account nonlinear effects, such as waveform steepening and variable-speed wave propagation, as well as molecular relaxation phenomena, ray tube spreading and atmospheric stratification.

The equation is given by:

$$\frac{\partial P}{\partial \sigma} = P\frac{\partial P}{\partial \tau} + \frac{1}{\Gamma}\frac{\partial^2 P}{\partial \tau^2} + \sum_\nu C_\nu \frac{1}{1+\theta_\nu \frac{\partial}{\partial \tau}}\frac{\partial^2 P}{\partial \tau^2} - \frac{1}{2G}\frac{\partial G}{\partial \sigma}P + \frac{1}{2\rho_0 c_0}\frac{\partial(\rho_0 c_0)}{\partial \sigma}P, \tag{1.1}$$

were $P = P(\sigma, \tau)$ is the dimensionless perturbation of the pressure distribution. The distance σ and time τ of the perturbation are also dimensionless. The operator appearing in the summation corresponds to the molecular relaxation, and it is equivalent to the following integral transform:

$$\frac{1}{1+\theta_\nu \frac{\partial}{\partial \tau}} f(\tau) = \frac{1}{\theta_\nu}\int_{-\infty}^{\tau} e^{(\xi-\tau)/\theta_\nu} f(\xi) d\xi,$$

with $f = \frac{\partial^2 P}{\partial \tau^2}$, in this case. Function $G(\sigma)$ denotes the ray-tube area, which can be evaluated assuming cylindrical or spherical wave propagation. The atmosphere conditions are given by density ρ_0, and speed of sound c_0, both being a function of the altitude. Other parameters include a dimensionless thermo-viscous parameter Γ, a dimensionless relaxation time θ_ν and dispersion parameter C_ν for each relaxation mode. Typically, there are two relaxation modes, one corresponding to the relaxation occurred in Oxygen molecules and the other one in Nitrogen ones. We refer to Section 4 for more details on the parameters used in the model.

The sonic-boom minimization problem we address here consists of, roughly, given a desired ground signature P^* and the distance of the propagation Σ –which is closely related to the altitude of the flight–, recovering the near-field signature that reproduces P^* as best as possible with regard to a norm. This is commonly formulated as an optimal control problem, through a least square approach [**17**], as follows:

$$\min_{P_0} \mathcal{S}(P_0) = \min_{P_0} \frac{1}{2}\int_{\mathbb{R}} \big(P(\Sigma, \tau) - P^*(\tau)\big)^2 d\tau. \tag{1.2}$$

Here P_0 lies in a set of admissible near-field signatures –which is usually constrained by the design variables associated to the geometry of the aircraft [**10, 17**]– and P is the solution of (1.1) with $P(\sigma_0, \tau) = P_0(\tau)$ for all $\tau \in \mathbb{R}$, where σ_0 would be the distance of the measure point in the near-field to the plane. The perceived loudness (PLdB) or the shock over-pressures are other functionals that are usually considered for minimization too [**10**].

1.3. Contents of the paper. The sonic-boom minimization problem involves various different time scales: the perturbation of the pressure takes place for less than half a second, while the propagation can last up to a minute, depending on the flight conditions [**16**]. As we shall see, this makes the computational treatment a hard task and motivates taking into account the large-time asymptotic behavior of

the employed numerical schemes because of its possible impact on the minimization process.

The connection between large-time behavior and the efficiency of the numerical minimization tools has been the object of earlier investigation. For instance, in [**1**], in the context of Burgers equation, it is shown that numerical schemes that do not behave correctly as time tends to infinity, may produce significant errors in the computation of minimizers for long-time horizon control problems.

Several analytical and numerical important issues arise in the context of the sonic-boom minimization problem. The large-time dynamics of solutions and its numerical counterparts is one of them. As we shall see, the asymptotic profile of solutions as $\sigma \to \infty$ is a gaussian, which is a manifestation of an asymptotic simplification towards a linear dynamics. But this is compatible with the intermediate asymptotics, given by the N-wave. In fact, for the viscous Burgers equation the N-wave endures for a time period of order $O(1/\varepsilon)$, ε being the viscosity coefficient [**7**]. Simulations show that the augmented Burgers equation exhibits a similar behavior, without contradicting the asymptotic result.

The rest of the paper is structured as follows. In Section 2 we describe the numerical methods that we use to solve (1.1)-(1.2). Then, in Section 3 we elaborate on some of the numerical difficulties one faces when dealing with optimal control problems for Burgers-like equations. Finally, in Section 4, we present a numerical simulation of the sonic-boom minimization problem (1.1)-(1.2) using realistic parameters.

2. Discretization of the augmented Burgers equation

For the numerical approximation of (1.1), we follow [**5, 17**], using a splitting method for each of the operators appearing in the equation. However, in our case we select Engquist-Osher for the nonlinear term, which has been shown to be appropriate for large-time evolution problems [**15**]. With respect to the optimization method, we opt for a conjugate gradient descent method. In particular, we adopt a continuous approach, based on the adjoint methodology. Let us remark that we pay special attention to the discretization and settings of the algorithm, as detailed in [**1**].

2.1. Optimization. In order to solve the optimal control problem (1.1)-(1.2), we resort to gradient-based techniques; in particular, to a conjugate gradient descent method (CG). We evaluate the gradient of the objective functional in (1.2) by means of the adjoint variable $Q(\sigma, \tau)$, which is governed by:

$$-\frac{\partial Q}{\partial \sigma} = -P\frac{\partial Q}{\partial \tau} + \frac{1}{\Gamma}\frac{\partial^2 Q}{\partial \tau^2} + \sum_{\nu} \frac{C_\nu}{1-\theta_\nu \frac{\partial}{\partial \tau}} \frac{\partial^2 Q}{\partial \tau^2} - \frac{1}{2G}\frac{\partial G}{\partial \sigma} Q + \frac{1}{2\rho_0 c_0}\frac{\partial(\rho_0 c_0)}{\partial \sigma} Q, \tag{2.1}$$

The adjoint equation is solved backward in σ, starting from the final propagation distance Σ to the initial distance σ_0. The initial condition provided to (2.1) is

$$Q(\Sigma, \tau) = P(\Sigma, \tau) - P^*(\tau).$$

In that case, $Q_0(\tau) = Q(\sigma_0, \tau)$ provides the gradient of the objective function in (1.2) with respect to $P_0(\tau)$.

2.2. Operator splitting. In solving forward augmented Burgers equation (1.1), or its corresponding adjoint equation (2.1), we employ operator splitting techniques. In this type of methods, the equation is decomposed into simpler subproblems corresponding to different terms generating the overall dynamics; each of them being handled independently by an appropriate discretization and numerical integration scheme.

For solving the diffusion subproblem, a central difference discretization is used, together with Crank-Nicolson integration:

$$\frac{P_j^{n+\frac{1}{5}} - P_j^n}{\Delta\sigma} = \frac{1}{\Gamma}\Big(\frac{\alpha}{\Delta\tau^2}\big(P_{j-1}^n - 2P_j^n + P_{j+1}^n\big) + \frac{1-\alpha}{\Delta\tau^2}\big(P_{j-1}^{n+\frac{1}{5}} - 2P_j^{n+\frac{1}{5}} + P_{j+1}^{n+\frac{1}{5}}\big)\Big),$$

where $\alpha \in [0,1]$. In our case, we take $\alpha = 1/2$.

Next, we adopt Engquist-Osher's scheme for discretizing the nonlinear term in (1.1), in combination with explicit Euler integration:

$$\begin{aligned}\frac{P_j^{n+\frac{2}{5}} - P_j^{n+\frac{1}{5}}}{\Delta\sigma} = \frac{1}{4\Delta\tau}\Big(&P_j^{n+\frac{1}{5}}(P_j^{n+\frac{1}{5}} - |P_j^{n+\frac{1}{5}}|) + P_{j+1}^{n+\frac{1}{5}}(P_{j+1}^{n+\frac{1}{5}} + |P_{j+1}^{n+\frac{1}{5}}|)\\ &- P_{j-1}^{n+\frac{1}{5}}(P_{j-1}^{n+\frac{1}{5}} - |P_{j-1}^{n+\frac{1}{5}}|) - P_j^{n+\frac{1}{5}}(P_j^{n+\frac{1}{5}} + |P_j^{n+\frac{1}{5}}|)\Big).\end{aligned}$$

Each of the relaxation terms is discretized independently using central differences, along with Crank-Nicolson integration:

$$\begin{aligned}&\frac{P_j^{n+\frac{3}{5}} - P_j^{n+\frac{2}{5}}}{\Delta\sigma} + \frac{\theta_{\nu_O}}{\Delta\tau}\Big(\frac{P_{j+1}^{n+\frac{3}{5}} - P_{j+1}^{n+\frac{2}{5}}}{\Delta\sigma} - \frac{P_{j-1}^{n+\frac{3}{5}} - P_{j-1}^{n+\frac{2}{5}}}{\Delta\sigma}\Big)\\ &\quad = C_{\nu_O}\Big(\frac{\alpha}{\Delta\tau^2}(P_{j-1}^{n+\frac{2}{5}} - 2P_j^{n+\frac{2}{5}} + P_{j+1}^{n+\frac{2}{5}}) + \frac{1-\alpha}{\Delta\tau^2}(P_{j-1}^{n+\frac{3}{5}} - 2P_j^{n+\frac{3}{5}} + P_{j+1}^{n+\frac{3}{5}})\Big),\end{aligned}$$

and

$$\begin{aligned}&\frac{P_j^{n+\frac{4}{5}} - P_j^{n+\frac{3}{5}}}{\Delta\sigma} + \frac{\theta_{\nu_N}}{\Delta\tau}\Big(\frac{P_{j+1}^{n+\frac{4}{5}} - P_{j+1}^{n+\frac{3}{5}}}{\Delta\sigma} - \frac{P_{j-1}^{n+\frac{4}{5}} - P_{j-1}^{n+\frac{3}{5}}}{\Delta\sigma}\Big)\\ &\quad = C_{\nu_N}\Big(\frac{\alpha}{\Delta\tau^2}(P_{j-1}^{n+\frac{3}{5}} - 2P_j^{n+\frac{3}{5}} + P_{j+1}^{n+\frac{3}{5}}) + \frac{1-\alpha}{\Delta\tau^2}(P_{j-1}^{n+\frac{4}{5}} - 2P_j^{n+\frac{4}{5}} + P_{j+1}^{n+\frac{4}{5}})\Big),\end{aligned}$$

where subindexes O and N stand for Oxygen and Nitrogen respectively. In both cases we choose $\alpha = 1/2$.

For the last two terms in (1.1), leading to ordinary differential equations, we simply perform analytical integration:

$$P_j^{n+1} = k^n P_j^{n+\frac{4}{5}}, \tag{2.2}$$

where k^n is the scaling factor due to the ray-tube spreading and atmospheric stratifications [**5**], given by

$$k^n = \sqrt{\frac{G(\sigma_n)}{G(\sigma_{n+1})}}\sqrt{\frac{\rho(\sigma_{n+1})c_0(\sigma_{n+1})}{\rho(\sigma_n)c_0(\sigma_n)}}.$$

We follow the same splitting process for the adjoint system (2.1).

3. Critical issues for the discrete methods

Optimal control problems like (1.1)-(1.2) are well-known to be extremely challenging from a numerical point of view. In fact, the nonlinearity is the dominant term and (1.1) exhibits a hyperbolic-like dynamics for large times, as we shall see.

3.1. Large-time dynamics. Motivated by the different time scales appearing in the dynamics of the sonic-boom phenomenon, in this section we analyze the large-time behavior of the augmented Burgers equation (1.1).

Note that equation (1.1) fits in the following type of equations:

$$\begin{cases} u_t = uu_x + \varepsilon u_{xx} + \sum_j c_j (K_{\eta_j} * u_{xx}) + (H(t))_t\, u, & (t,x) \in (0,\infty)\times\mathbb{R}, \\ u(0,x) = u_0(x), & x \in \mathbb{R}, \end{cases} \tag{3.1}$$

where

$$K_\eta(z) = \begin{cases} \dfrac{1}{\eta} e^{-z/\eta}, & z > 0, \\ 0, & \text{elsewhere.} \end{cases}$$

In fact, it is is enough to take $t = \Gamma^2(\sigma - \sigma_0)$, $x = \Gamma\tau$ and

$$P(\sigma,\tau) = \Gamma\, u(\Gamma^2(\sigma-\sigma_0), \Gamma\tau)$$

in (3.1), as well as $\varepsilon = 1/\Gamma$, $c_j = C_\nu$ and $\eta_j = \Gamma\theta_\nu$. Moreover, in our case, function H would be given by

$$H(t) = \ln \sqrt{\frac{\rho_0(\frac{t}{\Gamma^2}+\sigma_0)\, c_0(\frac{t}{\Gamma^2}+\sigma_0)}{G(\frac{t}{\Gamma^2}+\sigma_0)}}.$$

To analyze the large-time dynamics of these models, we remark that the change of variables $v = ue^{-H}$ transforms (3.1) into

$$\begin{cases} v_t = e^H v v_x + \varepsilon v_{xx} + \sum_j c_j (K_{\eta_j} * v_{xx}), & (t,x) \in (0,\infty)\times\mathbb{R}, \\ v(0,x) = v_0(x) = e^{-H(0)} u_0(x), & x \in \mathbb{R}. \end{cases} \tag{3.2}$$

A similar equation, with a constant coefficient as multiplicative factor of the nonlinearity, was already addressed in [**13**] where the authors proved the well-posedness of the Cauchy problem for L^1 initial data and obtained its large-time behavior.

The same arguments can be applied to (3.2) and, hence, also to (3.1). However, to do that, further assumptions are required regarding functions ρ_0, c_0 and G. If we assume that ρ_0 and c_0 are bounded from below and from above and that G corresponds to cylindrical or spherical waves (thus, $G_t/G = r/t$ with $r = 1/2$ for cylindrical waves and $r = 1$ for spherical ones), we can prove the following result.

THEOREM 3.1. *For any initial data $u_0 \in L^1(\mathbb{R})$, there exists a unique solution $u \in C([0,\infty), L^1(\mathbb{R}))$ of (3.1). Moreover, for any $p \in [1,\infty]$, u satisfies*

$$e^{-H(t)} t^{\frac{1}{2}(1-\frac{1}{p})} \|u(t) - e^{H(t)} v_M(t)\|_p \longrightarrow 0, \quad \text{as } t \to \infty,$$

where $v_M(t,x)$ is the solution of the following heat equation:

$$\begin{cases} v_t = (\varepsilon + \sum_j c_j) v_{xx}, & x \in \mathbb{R}, t > 0, \\ v(0) = M\delta_0. \end{cases} \tag{3.3}$$

Here δ_0 denotes the Dirac delta at the origin and M is the mass of the initial data, $M = \int_{\mathbb{R}} v_0(x)dx$.

SKETCH OF THE PROOF. The key point is that H is bounded from above for all $t \geq 0$ and that it goes to $-\infty$ as $t \to \infty$. Therefore, all the estimates obtained in [**13**] are applicable to this case. For the same reason, we can also apply the scaling procedure to obtain the asymptotic profile of (3.2). The only difference now is that the nonlinear term vanishes, since $e^H \to 0$ as $t \to \infty$. Thus, the equation for the first term in the asymptotic expansion is the heat equation. Moreover, reversing the change of variable $v = ue^{-H}$, we can obtain the large-time behavior of the solution u to (3.1). □

It is important to emphasize that, due to the range of parameters entering in (1.1), the diffusive profile v_M arising from (3.3) will not be achieved, the relevant time-horizon not being large enough, in realistic situations, in which N-waves are usually obtained. The coexistence of these two phenomena, N-waves versus for intermediate times and viscous waves for large times, was observed and analyzed in [**7**] in the context of the viscous Burgers equation

$$w_t = ww_x + \varepsilon w_{xx},$$

where it was observed that N-waves are intermediate metastable states that endure until $t = O(1/\varepsilon)$. Numerical experiments for (1.1) show that the behavior of its solutions is similar, being dominated by the nonlinear effects. As a matter of fact, Theorem 3.1 states that the molecular relaxation terms act as additional viscous terms as $t \to \infty$.

As we mentioned above, the range of parameters for (1.1) in the optimization problem under consideration, leads to a hyperbolic-like dynamics, while the other terms are still present. Thus, there are two key points that need to be taken into account at the numerical level:

- The nonlinear flux has to be discretized appropriately. Numerical fluxes that introduce too much numerical viscosity will affect, not only the accuracy of the forward problem, but the efficiency of optimization algorithms too (e.g. [**1, 13, 15**]).
- The molecular relaxation term behaves, as time tends to infinity, as an additional viscous term. Moreover, being a nonlocal operator, it has to be treated carefully to avoid undesired large-time effects [**13, 14**].

3.2. Drawbacks of the adjoint methodology and the least squares approach. In the context of the inviscid Burgers equation it is well known that (1.2) has multiple minimizers (see [**3**]). For instance, all three different initial conditions shown in Figure 2 give rise to the same solution at final time T, where a shock is present. In [**1**], the authors show that, among the various possible minimizers, the classical adjoint methodology tends to recover a compression wave in which the shock will not appear until the final time (Figure 2, top). The alternating descent method proposed in [**3**] leads to initial data that create the shock at the initial time (Figure 2, middle). Other strategies can also be defined so to have a shock arising at some intermediate instant (Figure 2, bottom).

In the viscous case (and also for (1.1)), the equation under consideration enjoys the property of backward uniqueness and, therefore, the lack of uniqueness for the optimization problem is no longer valid. Nevertheless, when the viscosity is small, at the numerical level, non-uniqueness issues still arise. Furthermore, the asymptotic simplification properties of Burgers-type equations for large times reduce the

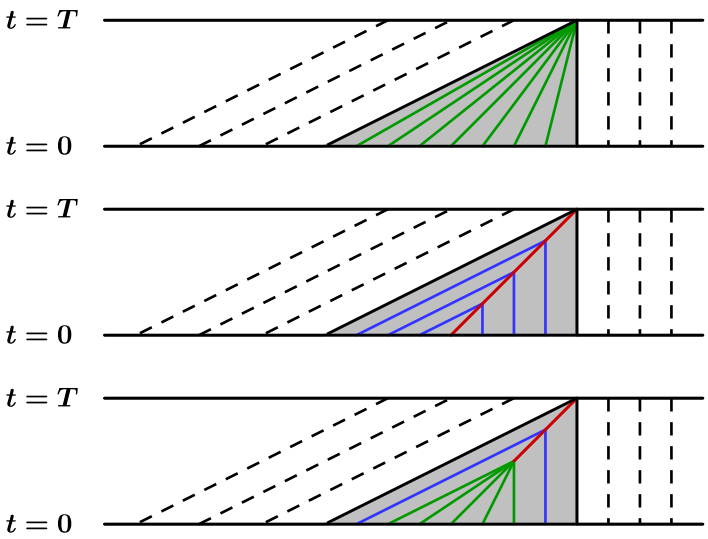

FIGURE 2. Different initial conditions which create the same target function with a shock at final time, T, for the inviscid Burgers equation: from a compression wave (top), from a shock at the initial data (middle) and from a shock that arises sometime in between (bottom).

sensitivity with respect to perturbations of the initial data. In Figure 3 we show two different initial data that lead to very similar profiles (up to an order of 10^{-6} in the L^2-norm of their distance). The smooth one has been obtained by means of an adjoint-based conjugate gradient method, following a discretize-then-optimize approach. Thus, the adjoint methodology is biased in preferring the smooth initial datum over some other possible minimizers.

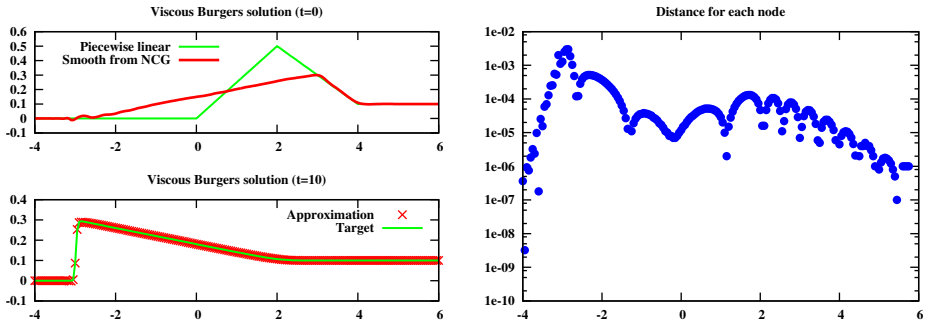

FIGURE 3. On the left, solutions of the viscous Burgers equation $u_t = uu_x + \nu u_{xx}$ with $\nu = 10^{-4}$ (bottom) for two different initial data (top). On the right, the L^2-norm of the difference of both solutions.

On the other hand, the strong time-irreversibility of viscous systems and the difficulty of recovering high-frequencies produces a second phenomenon that needs

to be handled. In the previous example we showed that two different initial data –the smooth one and the piecewise linear one– can produce very similar profiles. When using the adjoint method to compute the gradient of the functional, the viscous effects are enhanced. Thus, it is computationally expensive to recover initial data with peaks.

This pathology is very clear for the heat equation, where the influence of the nonlinearity is put aside. In Figure 4 we can observe that a target function that appears from a piecewise linear function is well reproduced by a smoother initial data. The latter has been computed using an adjoint-based conjugate gradient method, within a discretize-then-optimize approach.

In short, the presence of viscosity in the model desensitizes the least square objective functional to the presence of high frequency components in the initial data. This insensitivity or flatness of the objective functional with respect to high frequency components makes the optimization algorithm to be inefficient when trying to achieve singular minimizers.

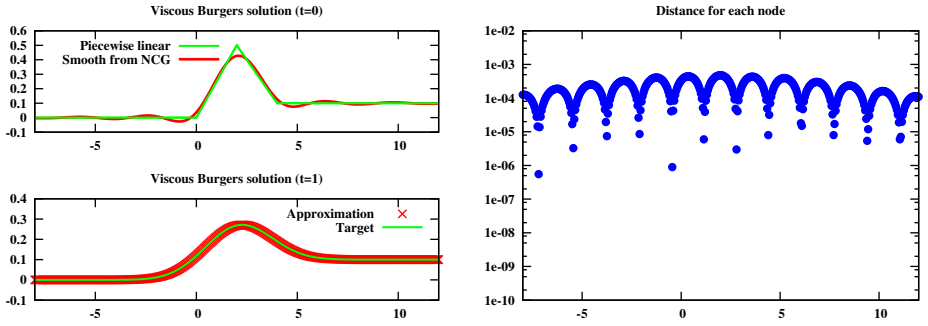

FIGURE 4. On the left, solutions of the heat equation $u_t = u_{xx}$ (bottom) for two different initial data (top). On the right, the L^2-norm of the difference of both solutions.

As we shall see in the next section, the problem of minimizing the sonic-boom within the class of F-function initial data exhibits similar symptoms.

4. Numerical results

In this section we discuss the numerical simulation of the sonic-boom minimization problem (1.1)-(1.2). In this test, we search for a near-field pressure giving rise to a prescribed far-field target. In doing so, we pick a target function which has not developed an N-wave. The target function we use for far-field is actually synthesized from the evolution of a known near-field. Furthermore, the target function under consideration is, indeed, a suitable one for the sonic-boom problem under consideration.

In practical applications, of course, the near-filed pressure depends on the geometry of the airplane. One of the common ways of representing the near-field pressure is using the F-function theory developed by Whitham (see [**10**] and the references therein). This theory stipulates that the near-field pressure can be approximated using F-functions, the Abel transform of the cross-sectional area of the

plane, $A(x)$:

$$F(x) = \frac{1}{2\pi} \int_0^x \frac{A''(\xi)}{\sqrt{x-\xi}}.$$

In F-function theory, the airplane's geometry is considered as a body of revolution along x-axis. Despite all inherent simplifications, the F-function theory provides a straightforward approach to identify the near-field when the geometry is known or, inversely, to approximate the optimal geometry when optimal near-field is given.

In Table 1, we collect the main parameters used to obtain the initial near-field pressure signature. We refer to [**10**] for detailed information on near-field calculation.

Mach number, M	2.7
Body length, L	91.5 m
Flight altitude, z	18288 m
Near-field distance measured from airplane, $r = 2L$	183 m

TABLE 1. Flight parameters to compute the near-field pressure from F-function (taken from [**10**]).

Now, regarding the physical parameters present in the ABE equation, we take $\Gamma = 8 \times 10^6$. The relaxation parameters are shown in Table 2. Density and speed of sound vary as a function of altitude. In Figure 5, we show the variation of density and speed of sound in the atmosphere. Moreover, we consider cylindrical ray-tube spreading [**5**], which implies that $G_\sigma/G = 1/(2\sigma)$. Note that the initial signature is measured at some distance from the plain and, thus, $\sigma_0 > 0$.

	Oxygen	Nitrogen
C_ν	1.7×10^{-5}	1.2×10^{-4}
θ_ν	4.6×10^{-8}	1.6×10^{-6}

TABLE 2. Parameters used for molecular relaxation (taken from [**5, 16, 17**]).

The minimizer we obtain is shown in Figure 6, as well as its corresponding signature at the ground level, in comparison with the exact solution. Even though, the final profile is closely matching the target function, the initial data are different. The obtained initial data lacks the peaks present in the original F-function. In other words, the L^2-norm used in the objective functional is not sensitive to high frequency modes in the near-field. This is due to the presence of viscosity in the model and the large-time evolution. We also observe the selective nature of the adjoint methodology when dealing with multiple solutions for inverse problems and its bias towards selecting smooth initial solutions.

5. Conclusions and future research

In this paper we implemented a least square approach to recover an admissible ground signature mitigating the sonic-boom. From a mathematical point of view, the accuracy of the obtained results is sufficient, as we were able to reproduce the

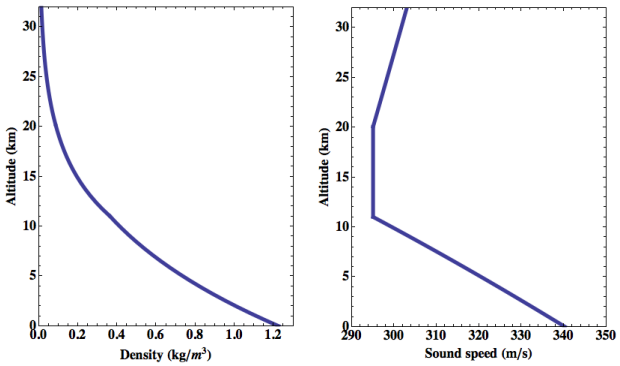

FIGURE 5. Density of the air (left) and sound speed (right) of the atmosphere [**5**].

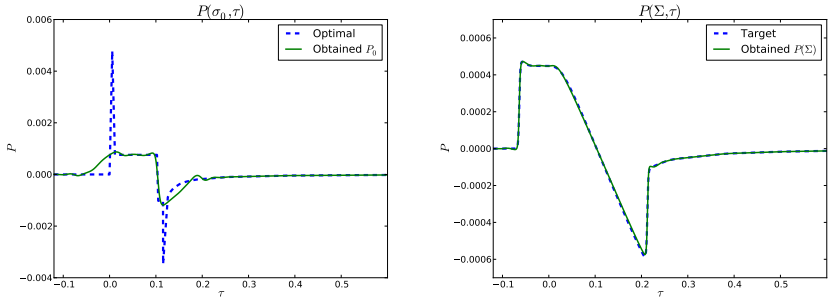

FIGURE 6. The solid green lines are the obtained minimizer (left) and its corresponding solution at the ground level (right). We compare them with the a-priori known optimal initial data and the corresponding target function it produces (blue dashed lines).

target function with a very high precision level. Moreover, we were able to handle efficiently the long time horizon that the propagation of the sonic-boom involves, which requires preserving the large-time asymptotic dynamics.

Nevertheless, further developments are required to obtain more satisfactory results in solving the sonic-boom minimization problem. In short, we identify two mayor drawbacks in our approach. On the one hand, the objective functional is highly insensitive to high frequency modes, which, indeed, is enhanced by the biased nature of the adjoint methodology. The preference for smooth initial solutions accentuates the difficulty of recovering F-functions as initial data both due to the diffusive term and the nonlinearity in the model.

One possible way of bypassing these difficulties would be to consider classes of parametrized initial data of F-function type, in contrast with the present work where we did not impose any restriction on the near-field signature. Another added remedy would be to consider functionals not only reproducing the ground signature, but also intermediate states.

References

1. Allahverdi, N., Pozo, A., and Zuazua, E. Numerical aspects of large-time optimal control of Burgers equation. *Submitted* (2014).
2. Alonso, J. J., and Colonno, M. R. Multidisciplinary optimization with applications to sonic-boom minimization. *Annual Review of Fluid Mechanics 44* (2012), 505–526.
3. Castro, C., Palacios, F., and Zuazua, E. An alternating descent method for the optimal control of the inviscid Burgers' equation in the presence of shocks. *Mathematical Models and Methods in Applied Sciences 18*, 3 (2008), 369–416.
4. Castro, C., Palacios, F., and Zuazua, E. Optimal control and vanishing viscosity for the Burgers equation. In *Integral Methods in Science and Engineering*, C. Costanda and M. E. Pérez, Eds., vol. 2. Birkhäuser Verlag, 2010, ch. 7, pp. 65–90.
5. Cleveland, R. O. *Propagation of sonic booms through a real, stratified atmosphere*. PhD thesis, University of Texas at Austin, 1995.
6. Hayes, W. D. *Linearized Supersonic Flow*. PhD thesis, California Institute of Technology, Pasadena, California, 1947.
7. Kim, Y. J., and Tzavaras, A. E. Diffusive N-waves and metastability in the Burgers equation. *SIAM Journal on Mathematical Analysis 33*, 3 (2001), 607–633.
8. Lions, J.-L., and Malgrange, B. Sur l'unicité rétrograde dans les problèmes mixtes paraboliques. *Mathematica Scandinavica 8* (1960), 277–286.
9. McLean, F. E. Some nonasymptotic effects on the sonic boom of large aircraft. Tech. Rep. D-2877, NASA, June 1965.
10. Minelli, A., el Din, I. S., and Carrier, G. Advanced optimization approach for supersonic low-boom design. In *18th AIAA/CEAS Aeroacoustics Conference (33rd AIAA Aeroacoustics Conference)* (Colorado Springs, CO, June 2012).
11. Ozcer, I. Sonic boom prediction using Euler/full potential methodology. In *45th AIAA Aerospace Sciences Meeting and Exhibit* (2007), Aerospace Sciences Meetings, American Institute of Aeronautics and Astronautics.
12. Pawlowski, J. W., Graham, D. H., Boccadoro, C. H., Coen, P. G., and Maglieri, D. J. Origins and overview of the shaped sonic boom demonstration program. Paper 2005-5, American Institute of Aeronautics and Astronautics, January 2005.
13. Pozo, A., and Ignat, L. I. A semi-discrete large-time behavior preserving scheme for the augmented Burgers equation. *Submitted* (2014).
14. Pozo, A., and Ignat, L. I. A splitting method for the augmented Burgers equation. *Submitted* (2014).
15. Pozo, A., Ignat, L. I., and Zuazua, E. Large-time asymptotics, vanishing viscosity and numerics for 1-D scalar conservation laws. *Mathematics of Computation*, to appear (2013).
16. Rallabhandi, S. K. Advanced sonic boom prediction using augmented Burger's equation. *Journal of Aircraft 48*, 4 (2011), 1245–1253.
17. Rallabhandi, S. K. Sonic boom adjoint methodology and its applications. In *29th AIAA Applied Aerodynamics Conference* (June 2011), American Institute of Aeronautics and Astronautics.
18. Whitham, G. B. The flow pattern of a supersonic projectile. *Communications on Pure and Applied Mathematics 5*, 3 (August 1952), 301–348.

New York City College of Technology
E-mail address: nh8@njit.edu

BCAM - Basque Center for Applied Mathematics
E-mail address: pozo@bcamath.org

BCAM - Basque Center for Applied Mathematics & Ikerbasque, Basque Foundation for Science
E-mail address: zuazua@bcamath.org